



**HAL**  
open science

## Numerical study of the effect of particle size dispersion on order within colloidal assemblies

Manuella Cerbelaud, Fabien Mortier, Hanady Semaan, Julien Gerhards,  
Benoit Crespin, Riccardo Ferrando, Arnaud Videcoq

► **To cite this version:**

Manuella Cerbelaud, Fabien Mortier, Hanady Semaan, Julien Gerhards, Benoit Crespin, et al.. Numerical study of the effect of particle size dispersion on order within colloidal assemblies. *Materials Today Communications*, 2024, 38, pp.107973. 10.1016/j.mtcomm.2023.107973 . hal-04385172

**HAL Id: hal-04385172**

**<https://hal.science/hal-04385172>**

Submitted on 10 Jan 2024

**HAL** is a multi-disciplinary open access archive for the deposit and dissemination of scientific research documents, whether they are published or not. The documents may come from teaching and research institutions in France or abroad, or from public or private research centers.

L'archive ouverte pluridisciplinaire **HAL**, est destinée au dépôt et à la diffusion de documents scientifiques de niveau recherche, publiés ou non, émanant des établissements d'enseignement et de recherche français ou étrangers, des laboratoires publics ou privés.

# Numerical study of the effect of particle size dispersion on order within colloidal assemblies

Manuella Cerbelaud<sup>a,\*</sup>, Fabien Mortier<sup>a</sup>, Hanady Semaan<sup>a,b</sup>, Julien Gerhards<sup>a</sup>, Benoit Crespin<sup>b</sup>, Riccardo Ferrando<sup>c</sup>, Arnaud Videcoq<sup>a</sup>

<sup>a</sup>*Univ. Limoges, CNRS, IRCER, UMR 7315, F-87000 Limoges, France*

<sup>b</sup>*Univ. Limoges, CNRS, XLIM, UMR 7252, F-87000 Limoges, France*

<sup>c</sup>*Physics Department, University of Genoa, Via Dodecaneso 33, 16146, Genoa, Italy.*

---

## Abstract

The formation of colloidal crystals is of interest in many fields, especially because of their optical properties. These properties are dictated by the colloidal arrangement. It is known that introducing particles with different size can change the structure of crystals and thus their resultant optical properties. To better understand how specific arrangements of particles can be obtained, a detailed understanding of the formation mechanisms is needed.

The influence of particle size distribution on the formation of colloidal crystals is studied by means of Brownian dynamics simulations performed with different types of interaction potentials. Crystal formation is first analyzed in systems containing homogeneous particles, then in systems with a size distribution.

It is shown that the interaction potential has a strong influence on the colloidal arrangement. For homogeneous particles, the width of the potential well affects the aggregate shape: a larger width leads to more elongated structures. When a size distribution is introduced, aggregation becomes more difficult, since the number of isolated colloids increases, and aggregates become disordered regardless the interaction potentials. Depending on the interaction potential, differences in the aggregates are observed. These differences are rationalized in terms of the specific features of the different potentials.

*Keywords:* Brownian dynamics simulation; colloidal crystal; size distribution; disordering

---

---

\*Corresponding author

*Email address:* manuella.cerbelaud@unilim.fr; Tel: +33 (0)5 87 50 23 47 (Manuella Cerbelaud)

## 1. Introduction

The understanding of the colloid behavior is important in many fields ranging from food industry to pharmacology and ceramics. To better understand this behavior, mesoscopic simulations using colloids as elemental entities can be performed. Numerous simulations have already been done for example in Brownian dynamics simulations [1, 2, 3, 4]. Generally, in such simulations, a homogeneous size is chosen for each kind of particles. However, experimentally, there is always a size distribution for the particles. To better understand how a size distribution can affect the results of simulations, it is proposed here to perform simulations for which ordering of colloids can be obtained.

Ordered aggregates or colloidal crystals have already been intensively studied because of their use in various fields ranging from optics to ceramics [5, 6, 7, 8, 9]. Numerous studies both experimental and numerical have shown that hard-sphere or repulsive colloids are able to form ordered structures when concentrated [5, 10, 11]. Experimentally, ordered structures can be obtained for example by sedimentation or by evaporative self assembly [12, 8]. More recently, it has also been shown that weakly attractive particles are also able to form ordered structures. For example, binary systems where particles interact via a weakly attractive potential can form colloidal crystals [13]. Another example is the possibility to order colloids modified by DNA via low energy attractive interactions [14]. From the point of view of numerical simulations, Bochicchio *et al.* have already shown that ordered aggregates can be observed with a weakly attractive potential based on the DLVO theory by choosing a well depth of around 3-4  $k_B T$  [15].

For colloidal crystals, structural defects have consequences for the desired properties. For example, defects can lead to a change in the reflective color of the crystals [16]. A key factor in minimizing the formation of defects is the use of homogeneous particle sizes. Nakawaga *et al.* have shown, that the crystallinity of the colloidal crystals they synthesize is strongly linked to the size uniformity of the nanoparticles used [17]. Disparity in size leads to a reduction in crystallinity. Liu *et al.* have studied in details the effect of particle size distribution on the formation of colloidal crystals based on polystyrene particles [18]. By adding irregularly sized particles to their system, they showed that crystallinity depends on both the concentration and size of the added particles. Modifying the size distribution of the particles enables them to control defects, which could be a way of controlling the optical properties of the resulting

32 crystals.

33 In this paper, we propose to study the effect of particle size inhomogeneity in Brownian  
34 dynamics simulations. To this end, we focus on a system similar to that studied by Bochi-  
35 chio *et al.*, which features particles interacting with weakly attractive interaction potentials  
36 and capable of forming ordered aggregates [15]. First, we will analyze how aggregates are  
37 ordered when all particles have the same size, as a function of different interaction potentials.  
38 Then we will analyze how particle size distribution modifies the simulation results focusing  
39 in particular on the organization of aggregates.

## 40 2. Simulation methods

41 In this paper, the aggregation and organization of colloids subjected to low-intensity at-  
42 tractive interactions is studied. The effect of two kinds of interaction potentials is analyzed:  
43 the DLVO potential [19] and the generalized Lennard Jones potential [20].

44 The system used in this paper is similar to the one presented in reference [15]. Alumina par-  
45 ticles with a mean radius of  $a = 250$  nm suspended in water are considered. The interaction  
46 between particles will first be modeled using a DLVO potential. This potential is composed  
47 of an attractive part due to van der Waals forces and a repulsive part due to electrostatic  
48 repulsion. The van der Waals component can be expressed as [19]:

$$U_{ij}^{\text{vdW}}(r_{ij}) = -\frac{A}{6} \left[ \frac{2a_i a_j}{r_{ij}^2 - (a_i + a_j)^2} + \frac{2a_i a_j}{r_{ij}^2 - (a_i - a_j)^2} + \ln \left( \frac{r_{ij}^2 - (a_i + a_j)^2}{r_{ij}^2 - (a_i - a_j)^2} \right) \right], \quad (1)$$

49 where  $A$  is the Hamaker constant (here  $A = 4.76 \times 10^{-20}$  J)[21],  $a_i$  the radius of particle  $i$  and  
50  $r_{ij}$  the distance between particles  $i$  and  $j$ . The electrostatic repulsion is described by [22]:

$$U_{ij}^{\text{el}}(r_{ij}) = 2\pi\epsilon \frac{a_i a_j}{a_i + a_j} \psi^2 \left[ \ln \left( \frac{1 + e^{-\kappa h_{ij}}}{1 - e^{-\kappa h_{ij}}} \right) + \ln (1 - e^{-2\kappa h_{ij}}) \right], \quad (2)$$

51 where  $\psi$  is the surface potentials of the particles,  $\epsilon = \epsilon_0 \epsilon_r$  the dielectric constant of the solvent  
52 (here  $\epsilon_r = 81$ ), and  $\kappa$  the inverse Debye screening length. In the following,  $\psi = 0.1$  V and  
53  $\kappa = 2.8 \times 10^8$  m $^{-1}$  are used. The well depth of the interaction potential is then  $3.3 k_B T$ , with  
54  $k_B$  the Boltzmann constant and  $T$  the temperature (here  $T = 293$  K). This value allows us to  
55 observe the organization of aggregates [15]. A plot of this potential is shown in Figure 1(a).

56 The well depth of the DLVO potential is size dependant. If the interacting particles are

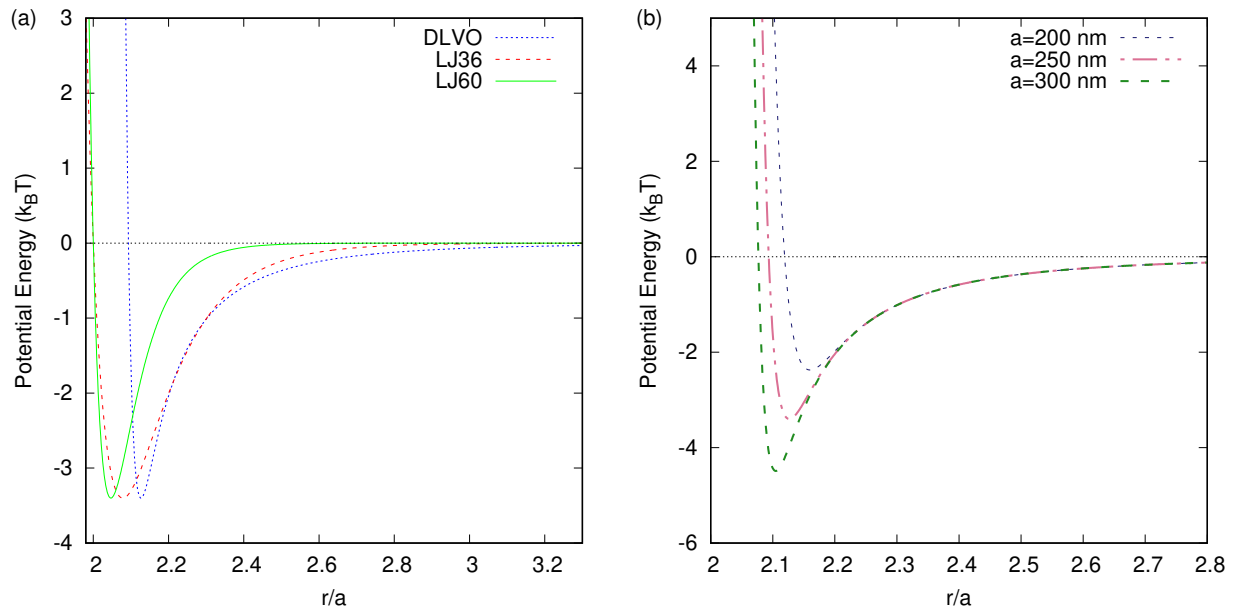


Figure 1: a) Interaction potentials in units of  $k_B T$  as a function of distance between particles. (b) DLVO potential in units of  $k_B T$  as a function of distance between particles for particles of size 200, 250 and 300 nm.

57 larger, the potential well becomes deeper. Conversely, for interactions between smaller par-  
 58 ticles, the well is shallower (see plots of DLVO potential with  $a = 200$  nm and  $a = 300$  nm in  
 59 Figure 1(b)).

60

61 The aggregation obtained using the DLVO potential will be compared to those obtained  
 62 using a generalized Lennard Jones potential defined as follows:

$$U_{ij}^{\text{LJ}}(r_{ij}) = 4\epsilon \left[ \left( \frac{a_i + a_j}{r_{ij}} \right)^n - \left( \frac{a_i + a_j}{r_{ij}} \right)^{n/2} \right] \quad (3)$$

63 with  $\epsilon$  the well depth. The value of  $n$  influences the shape and the range of the interaction  
 64 potential. Initially  $n=36$  will be used, as it has already been done in a previous work [20].  
 65 This value allows us to obtain the same range of interaction as for the DLVO potential, that  
 66 means that particles will interact over similar approach distances. However, the width of  
 67 the potential well depth is larger than that of the DLVO potential. As a comparison,  $n=60$   
 68 will also be used, which gives a width of well depth similar to that of DLVO potential. In  
 69 this case, the range of interaction will be shorter. In order to compare only the impact of  
 70 the shape of the potential, all the simulations are carried out with  $\epsilon = 3.3 k_B T$  which is the  
 71 value of the DLVO potential well depth for particles with  $a = 250$  nm. Thereafter, LJ36 and

72 LJ60 refer to simulations carried out with  $n=36$  and  $n=60$  respectively. In contrast to the  
73 DLVO potential, the potential well depth of LJ36 or LJ60 do not vary with particle size. The  
74 different potentials used in this study are shown in the Figure 1(a). All the potentials will  
75 be cut at  $r_{ij} = r_c = 1.15(a_i + a_j)$ .

76

77 Brownian dynamics simulations are performed with 10,000 particles in a cubic box with  
78 periodic conditions. Initially, particles are randomly distributed in the simulation box. The  
79 size of the box is defined so that the volume fraction of particles is equal to 6%. To understand  
80 the influence of particle size dispersion on aggregation, a particle size distribution is intro-  
81 duced by randomly choosing the particle size in a normal distribution with mean  $a = 250$  nm  
82 and standard deviations ranging from  $0.01a$  to  $0.1a$ . More specifically, the distribution effect  
83 with a standard deviation of  $0.01a$ ,  $0.025a$ ,  $0.05a$  and  $0.1a$  will be studied. One condition  
84 to use the Brownian dynamics simulations is to choose a time step being higher than the  
85 velocity relaxation time of each particle, while being also sufficiently small to ensure that the  
86 interaction forces do not change significantly during one integration step [2]. To satisfy these  
87 conditions, it was chosen to restrict the particle size between  $0.8a$  and  $1.2a$ . Examples of the  
88 size distributions used in simulations for the different standard deviations mentioned before  
89 are shown in Figure 2. In the following, simulations carried out with a standard deviation of  
90  $0.01a$ ,  $0.025a$ ,  $0.05a$  and  $0.1a$  will be denoted by  $\sigma = 0.01$ ,  $0.025$ ,  $0.05$  and  $0.1$ , respectively.  
91 The time step of the simulations has been fixed at  $1.5 \times 10^{-7}$  s. Simulations have been per-  
92 formed with different home-made simulations codes running on CPU or on GPU based on  
93 OPENCL [23] or on CUDA. Results are averaged over three independant simulations.

94

### 95 **3. Results and discussion**

#### 96 *3.1. Aggregation without size dispersion*

97 First, the aggregation without size dispersion is analyzed. Snapshots of Brownian dy-  
98 namics simulations obtained at  $t = 300$  s are shown in Figure 3.

99 Whatever the interaction potential used, the aggregates are organized and isolated parti-  
100 cles remain. To quantify the organization, order parameters P12 indicating the percentage of  
101 particles with 12 first neighbors and P6 indicating the percentage of particles with 6 second

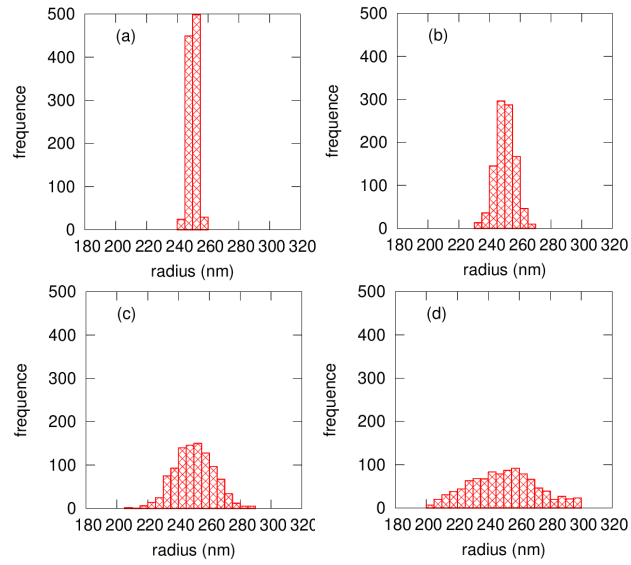


Figure 2: Examples of the size distributions used in simulations for the different standard deviations: (a)  $\sigma = 0.01$ , (b)  $\sigma = 0.025$ , (c)  $\sigma = 0.05$  and (d)  $\sigma = 0.1$ .

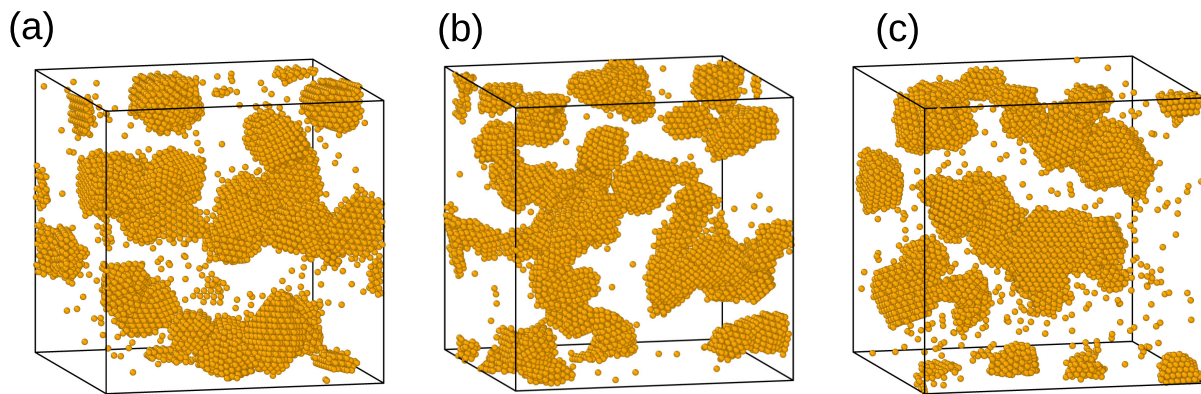


Figure 3: Snapshots of Brownian dynamics simulations at 300s: (a) DLVO, (b) LJ36 and (c) LJ60.

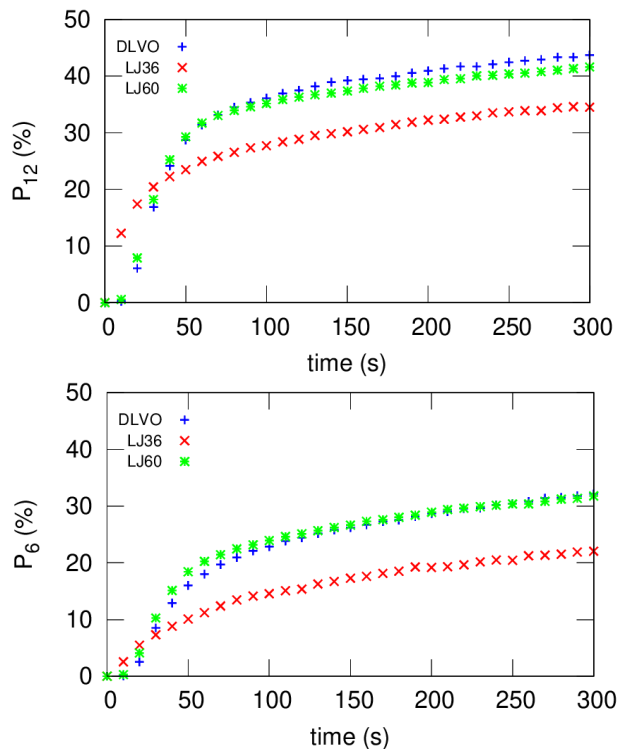


Figure 4: Evolution in time for the two order parameters  $P_{12}$  and  $P_6$  obtained for the different potentials DLVO, LJ36 and LJ60.

102 neighbors are analyzed (see Figure 4). The distance used to identify the first and second  
 103 neighbors are based on an analysis of the radial distribution functions.

104 In all cases,  $P_{12}$  and  $P_6$  increase during the simulations confirming an ordering in the  
 105 simulation. The values seem to indicate that order is more important in the aggregates  
 106 obtained with the DLVO and LJ60 potentials than with the LJ36 potential. On the other  
 107 hand, the shape of the aggregates obtained is different for LJ36 compared to DLVO and LJ60  
 108 (see Figure 5). The aggregates obtained with LJ36 are more elongated.

109 The aggregates obtained with LJ36 are the result of the coalescence of smaller aggre-  
 110 gates that seem to rearrange little into a compact shape. Various tests are carried out to  
 111 understand this difference in organization. Previous studies have shown that the ability of  
 112 an aggregate to reorganize may be linked to the ability of the particles to detach [15]. To  
 113 examine this property with different potentials, simulations are carried out to quantify the  
 114 average dissociation time of a dimer. To do this, Brownian dynamics simulations are carried  
 115 out by considering only two particles initially placed so that their separation distance is that  
 116 of the minimum of the interaction potential. The dissociation time corresponds to the time

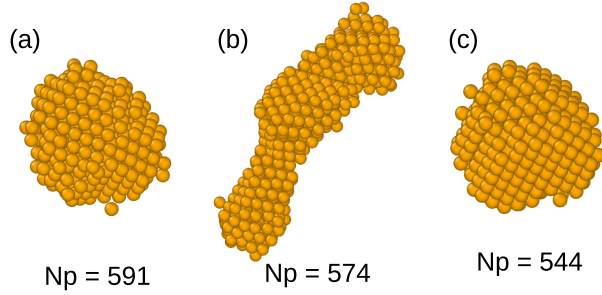


Figure 5: Snapshots of representative isolated aggregates obtained at 300 s in Brownian dynamics simulations: (a) DLVO, (b) LJ36 and (c) LJ60.  $N_p$  is the number of particles in the aggregates.

117 taken for the particles to stop interacting, i.e. the time required for them to be at a separa-  
 118 tion distance greater than  $3.3a$ . The average dissociation time obtained over 200 simulations  
 119 was measured at  $t = 6.42 \times 10^{-2}$  s,  $t = 8.93 \times 10^{-2}$  s and  $t = 3.02 \times 10^{-2}$  s respectively for  
 120 DLVO, LJ36 and LJ60. The dissociation times are lower for the latter potential, indicating a  
 121 greater ability of the particles to dissociate in these systems, allowing the aggregates to locally  
 122 reorganize better. However, the dissociation times obtained with LJ36 and DLVO are not  
 123 so different and do not fully explain the difference in aggregate shape. The main difference  
 124 between these two potentials is the width of the well depth, which is larger for LJ36. Because  
 125 of the potential width, not only neighbor particles but also second neighbors may play a role  
 126 in the ordering. The second-neighbor interactions on nucleus has thus been investigating by  
 127 analyzing the energy of a compact aggregate made up of 13 particles (icosaedre) during a  
 128 Brownian dynamics simulations. This structure has been chosen because it is compact and  
 129 can be considered as a first nucleus. Results show that the energy of the system is lower  
 130 when using LJ36 than when using DLVO or LJ60. The lowest energy obtained in DLVO is  
 131  $-199.6 k_B T$ , in LJ60  $-203.2 k_B T$  and in LJ36  $-227.0 k_B T$ . As already discussed, this differ-  
 132 ence can be attributed to the interaction width of the LJ36 potential well depth. Since this  
 133 width is larger than that of the two other potentials, with LJ36 the second neighbors will  
 134 also interact and organize themselves locally to minimize the total energy of the aggregate.  
 135 As a consequence with this potential, nuclei may form more easily and have a sufficiently low  
 136 energy to allow rapid crystal growth. Once the crystal nuclei are formed, aggregates continue  
 137 to grow by coalescence, resulting in the formation of elongated aggregates. The narrower well  
 138 depth of the LJ60 and DLVO potential wells, on the other hand, makes the reorganization of

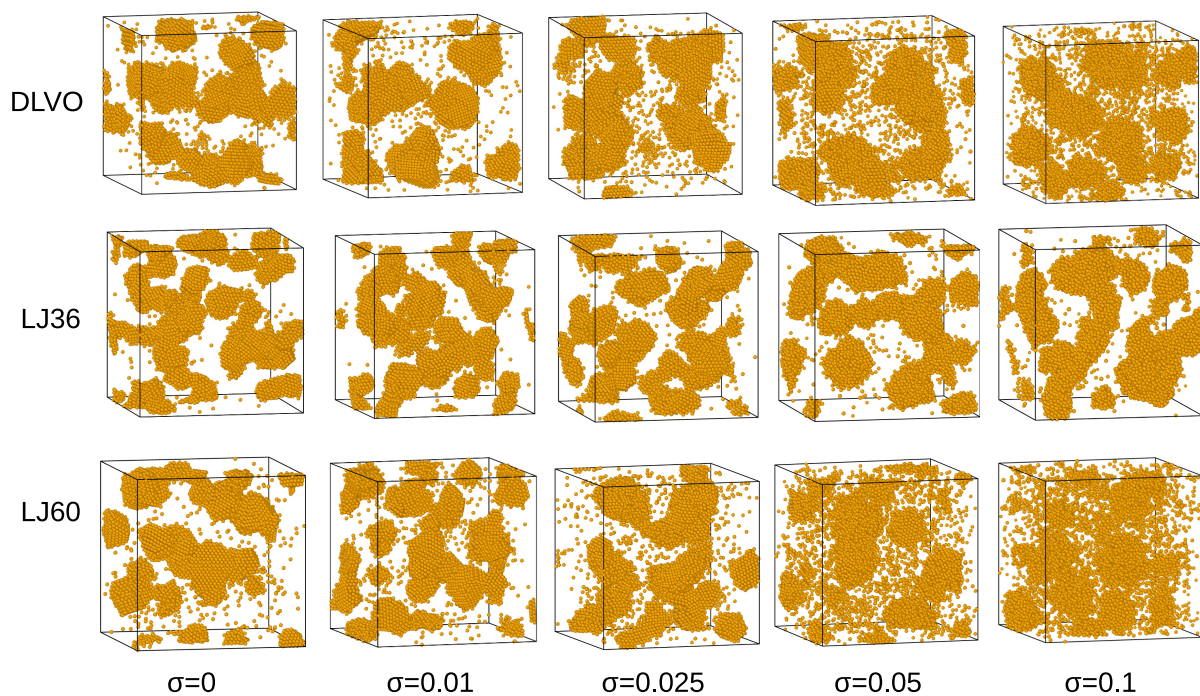


Figure 6: Snapshots of simulations at  $t = 300$ s as a function of the radius dispersion: first row: DLVO potential, second row: LJ36 potential and third row: LJ60 potential.

139 aggregates more difficult, and the nuclei should be less energetically stable. Nuclei should be  
 140 more difficult to stabilize, leading to later crystallization (see Figure 4). At the initial stage  
 141 of aggregation, the P6 and P12 parameters increase indeed faster for LJ36 than for LJ60 and  
 142 DLVO. In summary, the LJ60 and DLVO potentials, which have similar well potentials in  
 143 terms of well value and width, give similar simulation results. On the other hand, the LJ36  
 144 potential results in a different aggregation which can be explained by a larger potential well  
 145 width.

### 146 3.2. Aggregation with size dispersion

147 Experimentally, particles are always dispersed in size. Studies have already shown that  
 148 differences in particle size lead to changes in crystallization. To understand the impact  
 149 of particle size dispersion in the previous simulations, the simulations were repeated with  
 150 particle sizes varying according to a Gaussian distribution. The results obtained are shown  
 151 in Figures 6 and 7.

152 For the dispersion  $\sigma = 0.01$ , there is no significant effect on the aggregates' organization.

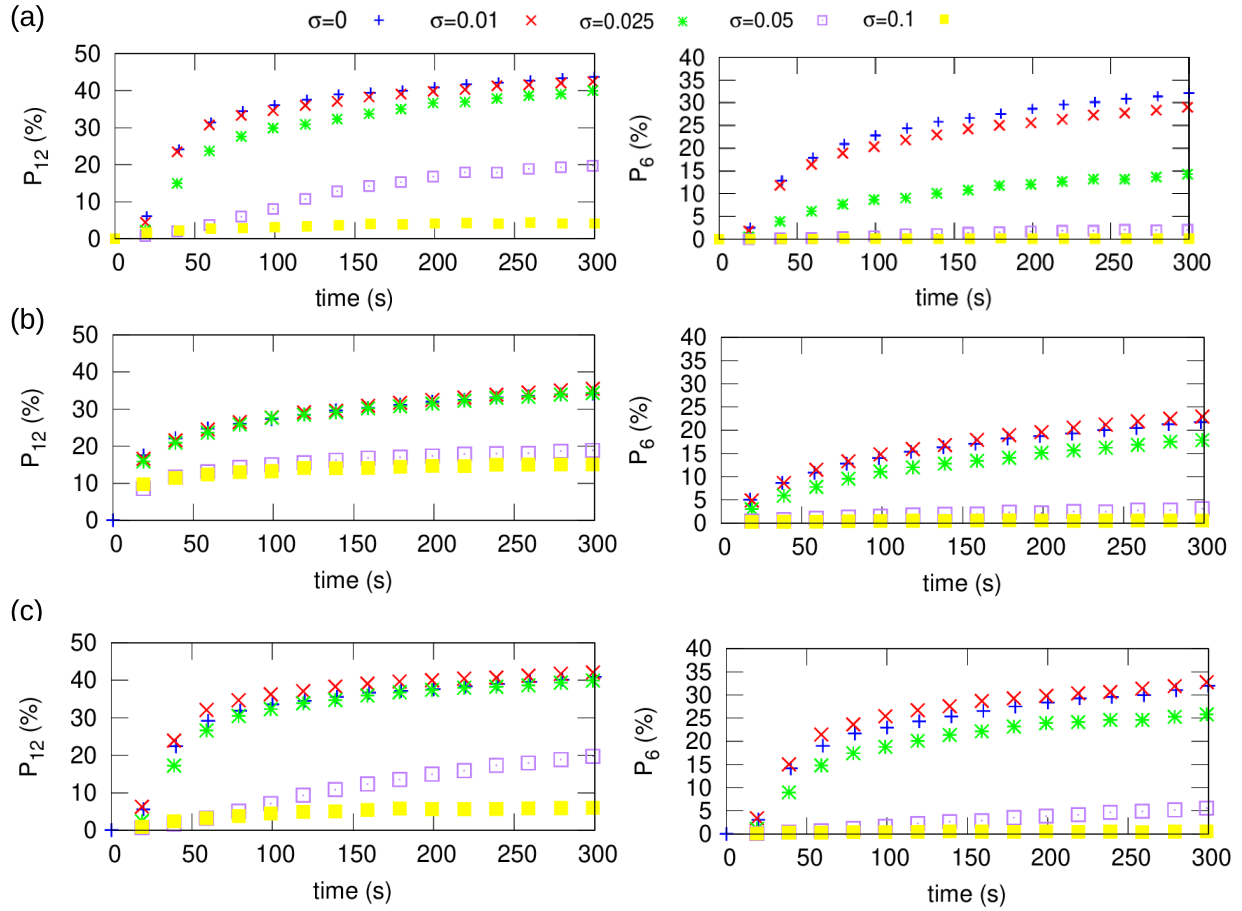


Figure 7: Evolution in time for the two order parameters  $P_{12}$  and  $P_6$  obtained with different radius distribution for : (a) DLVO potential, (b) LJ36 potential and (c) LJ60 potential.

153 Aggregates can accommodate the small size variations. However, whatever the interaction  
 154 potentials used, results show that the aggregates become disordered with a dispersion greater  
 155 than or equal to  $\sigma = 0.05$ . This observation is in agreement with experiments, which demon-  
 156 strate that size dispersion leads to disorganized aggregates [17]. As for  $\sigma = 0.025$ , there is  
 157 a difference between the potentials. According to the analyses of P6 parameters, with this  
 158 dispersion, aggregates obtained with DLVO seem more disordered than the ones obtained  
 159 with the two kinds of generalized Lennard Jones potentials. Given that the size distributions  
 160 are the same in the different simulations, this observation is due to the interaction potential.  
 161 When the size dispersion increases, an increase in the number of isolated particles is also  
 162 observed, whatever the potential (see Table 1). An analysis of the average size of the isolated  
 163 particles shows that their average radius is smaller than that of the distribution ( $a = 250$  nm).

Table 1: Averaged number of isolated particles  $n_{isolated}$  and averaged radius of isolated particles  $a_{isolated}$  observed in Brownian dynamics simulation at  $t = 300$  s for the different interaction potentials. Results are averaged over three independant simulations

	DLVO		LJ36		LJ60	
distribution	$n_{isolated}$	$a_{isolated}$ (nm)	$n_{isolated}$	$a_{isolated}$ (nm)	$n_{isolated}$	$a_{isolated}$ (nm)
$\sigma = 0$	321.7	250.0	61.3	250.0	346.3	250.0
$\sigma = 0.01$	310.0	249.8	72.3	249.5	384.0	249.9
$\sigma = 0.025$	534.7	248.5	118.3	249.4	630.3	249.7
$\sigma = 0.05$	1039.7	246.5	210.0	247.8	1426.3	247.5
$\sigma = 0.1$	1416.0	232.5	210.0	249.5	1624.3	246.6

164

165 Figure 8 shows the percentage of isolated particles as a function of their size in the case  
 166  $\sigma = 0.1$ . For the two generalized Lennard Jones potentials, the percentage of isolated particles  
 167 decreases slightly with the size of particles. However, for the simulation with the DLVO  
 168 potential, it is clearly observed that the smallest particles are more isolated than the largest  
 169 ones. These evolutions are in agreement with the observation of the average radius of isolated  
 170 particles. The decrease in the percentage of isolated particles with their size suggests that  
 171 regardless of the potential used, the smallest particles have more difficulty to aggregate and  
 172 remain more isolated. This can explain the increase of the number of isolated particles with

173 the increase in size dispersion. Indeed, whatever the interaction potential used, an increase  
174 in size dispersion leads to an increase in the number of smaller-than-average particles, which  
175 will have more difficulty in aggregating and thus will tend to remain isolated. Different  
176 reasons could explain this phenomenon. First, smallest particles, because of their smaller  
177 mass, could have a higher vibration frequency in the well and escape more easily from the  
178 potential well depth and therefore not be bound. Moreover, because of their size, small  
179 particles are more difficult to bind to several other particles. Insertion of small particles  
180 into an aggregate could also create geometric constraints, which results in larger network  
181 distortions often less stable. It has already been shown experimentally that the insertion of  
182 small particles of irregular size leads to more disordered structures than larger particles [18].  
183 This should lead to a preferential localization of small particles on the surface of aggregates,  
184 or even to their isolation, to minimize distortion and therefore the system energy.  
185 However, it can be noted that the smallest particles are more isolated when using the DLVO  
186 potential. This can be explained because the DLVO interaction is size dependant and when  
187 the particle become smaller, they interact by a shallower potential well (see Figure 1(b)).  
188 The decrease of the well depth makes the bonding of small particles less stable compared  
189 to the other potentials, resulting in more small particles remaining isolated with the DLVO  
190 potential.

191 Let's now look at how size distribution affects the distribution of particles in aggregates.  
192 This analysis is carried out more specifically on systems with  $\sigma = 0.1$ . In the Figure 9a,  
193 isolated aggregates are represented with particles colored according to their radius. The  
194 images in the top row show the aggregate from the front, allowing us to analyze the aggregate  
195 surface. To better understand the distribution of particles within the aggregates, cross-  
196 sections are also shown below. In the case of the DLVO potential, there are fewer large  
197 particles on the surface than with the generalized Lennard Jones potentials (see red or orange  
198 particles in Figure 9a). On the other hand, particles with the largest radii are clearly present  
199 at the cross-sectional level. To better quantify this, the number of coordination of the  
200 aggregated particles as a function of their radius is reported in Figure 9b. The general trend  
201 is an increase of the coordination number with the radius of particles. Geometrically, larger  
202 particles are likely to have more neighbors than smaller ones. However, it can be noticed that  
203 the curves for LJ potentials do not show a monotonic increase, while the trend observed for

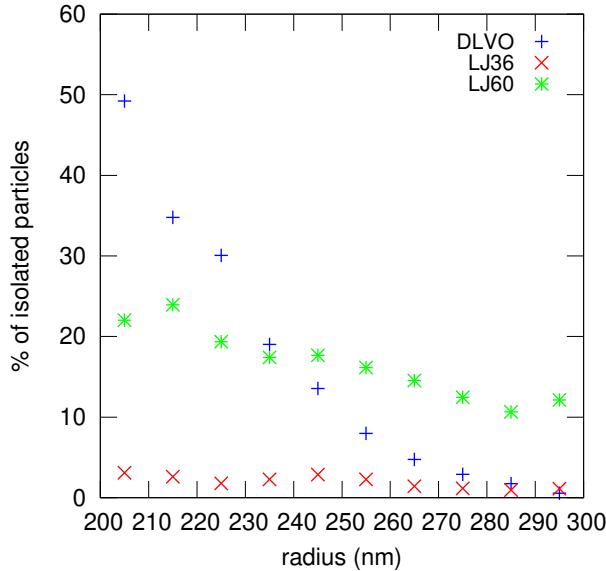


Figure 8: Percentage of isolated particles as a function of size at  $t = 300$  s for  $\sigma = 0.1$ . Results are obtained on one simulation. The percentage is expressed as the ratio of the number of isolated particles with a size within the interval under consideration to the total number of particles with a size within this interval.

204 DLVO is continuous and monotonic. For DLVO potential, the larger the particle radius is, the  
 205 greater is the coordination number. This is consistent with the fact that large particles are  
 206 located preferably inside the aggregates. The curves of the coordination numbers show also  
 207 that the trend is less pronounced for the generalized Lennard Jones potentials and particles  
 208 of different sizes are better distributed in the aggregates.

209 According to these results, including a size distribution has not exactly the same effect  
 210 when using the DLVO or the generalized Lennard Jones potentials. The difference can  
 211 be explained by the dependency of the well depth with the size of particles. As already  
 212 mentioned, for the Lennard Jones potentials, changing the sizes of particles has indeed no  
 213 effect on the interaction potential. The effect of size dispersion can be explained only by  
 214 geometrical constraints and by the higher mobility of small particles. However, as already  
 215 mentioned the DLVO potential is size dependant and when particles size increases, the well  
 216 becomes deeper (see Figure 1(b)). To reduce the energy of the system, with the DLVO  
 217 potential, it is then better to have aggregation between the largest particles. Thus, the biggest  
 218 particles will tend to aggregate together with the maximum compacity and the smallest ones  
 219 will essentially be expelled from the aggregate center and even detached. This will result

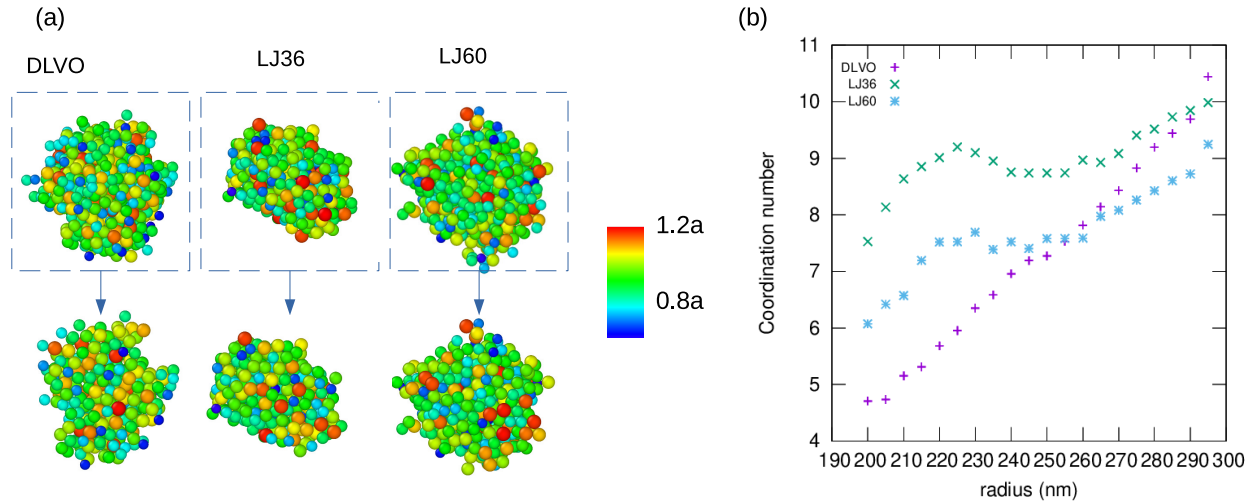


Figure 9: (a) Snapshots of an isolated aggregate obtained in simulations at  $t = 300$  s for  $\sigma = 0.1$ : on the top aggregate seen from front and below, cross-section of the aggregate. Particles are colored according to their radius. (b) Coordination number of particles in aggregates as a function of their radius at  $t = 300$  s for  $\sigma = 0.1$ . Results are averaged over 3 simulations.

220 in a different distribution of particles in the system to that observed with the generalized  
 221 Lennard Jones potentials. As already mentioned, Figure 7 shows that aggregates obtained for  
 222  $\sigma = 0.025$  are more disordered with the DLVO potential than with the generalized Lennard  
 223 Jones potentials. This can also be explained by the interactions between particles. According  
 224 to Figure 1(b), the separation distance where is found the minimum of well depth of DLVO  
 225 potential, decreases with the size of particles. In that case, even if the size of particles is  
 226 not so different ( $\sigma < 0.05$ ), when aggregating, larger particles will tend to approach more  
 227 each other. This will cause some distortions in the particle network and render more difficult  
 228 the ordering and the values of the order parameters will decrease. On the contrary, particles  
 229 interacting with the generalized Lennard Jones potentials will be able to maintain an ordered  
 230 network until the size dispersion implies geometrical constrains because they will stay at the  
 231 same distance.

232 These results show that to understand the effect of size distribution in real systems, it is  
 233 important to describe the interactions between particles accurately, as they can be size-  
 234 dependent and consequently induce different behaviors.

## 235 4. Conclusion

236 In this paper, crystallization using attractive potentials is analyzed. First, aggregation  
237 between homogeneous particles interacting via different potentials having the same well depth  
238 values are studied. It has been shown that the width of the interaction potential well depth  
239 has consequences for the shape and degree of organization of the aggregates. A narrow well  
240 depth results in more spherical and organized aggregates. A larger width, on the other hand,  
241 produces more elongated aggregates. A larger well depth seems to facilitate the formation  
242 of nuclei, resulting in numerous small organized aggregates forming and then coalescing to  
243 form larger elongated aggregates.

244 Next, the effect of introducing size dispersion was analyzed. In all cases, size dispersion led  
245 to the disorganization of the aggregates and an increase in the number of isolated particles.  
246 Aggregates obtained with  $\sigma \geq 0.05$  are all disordered regardless the potential used. This  
247 result is in agreement with the results found in literature showing that particles of irregular  
248 size affect the microstructure of colloidal crystals [16, 18, 17]. However, the study also shows  
249 that the interaction potentials between the colloids can affect differently the distribution  
250 of particles both in aggregates and in isolated particles. There is a non trivial effect of  
251 the interaction potentials. Interaction potentials that give similar results with particles of  
252 identical size may give indeed different results when a particle size distribution is introduced.  
253 The difference is explained by a change of the potential well depth as a function of particle  
254 size.

255 To conclude, this study opens new perspective to control defects in the crystal and therefore  
256 their properties by modifying the interactions between particles. From a more general point  
257 of view, it also shows that results of simulations can be impacted by a size distribution.  
258 Depending of the properties studied numerically, it can thus be necessary to consider a size  
259 dispersion, which is always present in experiments.

## 260 CRediT author statement

261 **Manuella Cerbelaud**: Conceptualization, Software, Investigation and Formal analysis;  
262 **Fabien Mortier**: Investigation and Formal analysis; **Hanady Semaan**: Investigation;  
263 **Julien Gerhards**: Software; **Benoit Crespin**: Software; **Riccardo Ferrando**: Formal  
264 analysis and **Arnaud Videcoq**: Conceptualization and Formal analysis.

265 All authors contributed to writing the paper.

## 266 **Acknowledgments**

267 This research was funded, in whole or in part, by l'Agence Nationale de la Recherche  
268 (ANR), project ANR-20-CE46-0004. Authors thank also the Région Nouvelle Aquitaine for  
269 the cofunding of the SOMA-DNS project and the National Research Agency for an insti-  
270 tutional grants under the Investments for the future program with the reference ANR-18-  
271 EURE-0017 TACTIC.

272 Figures 3, 5, 6, and 9 have been obtained by OVITO [24].

## 273 **References**

- 274 [1] E. Dickinson, S. Krishna, Aggregation in a concentrated model protein system: a meso-  
275 scopic simulation of  $\beta$ -casein self-assembly, *Food Hydrocolloids* 15 (2) (2001) 107–115.  
276 doi:[https://doi.org/10.1016/S0268-005X\(00\)00057-6](https://doi.org/10.1016/S0268-005X(00)00057-6).
- 277 [2] M. Cerbelaud, A. Videcoq, P. Abélard, C. Pagnoux, F. Rossignol, R. Ferrando, Heteroag-  
278 gregation between  $\text{Al}_2\text{O}_3$  submicrometer particles and  $\text{SiO}_2$  nanoparticles : Experiments  
279 and simulation, *Langmuir* 24 (2008) 3001–3008. doi:[doi.org/10.1021/la702104u](https://doi.org/10.1021/la702104u).
- 280 [3] M. Piechowiak, A. Videcoq, F. Rossignol, C. Pagnoux, C. Carrion, M. Cerbelaud,  
281 R. Ferrando, Oppositely charged model ceramic colloids: Numerical predictions and  
282 experimental observations by confocal laser scanning microscopy, *Langmuir* 26 (2010)  
283 12540–12547. doi:[doi.org/10.1021/la101027d](https://doi.org/10.1021/la101027d).
- 284 [4] R. Delacruz-Araujo, D. Beltran-Villegas, R. Larson, U. Cordova-Figueroa, Rich  
285 janus colloid phase behavior under steady shear, *Soft Matter* 12 (2016) 40.71–4081.  
286 doi:[10.1039/C6SM00183A](https://doi.org/10.1039/C6SM00183A).
- 287 [5] E. A. Barringer, H. K. Bowen, Formation, packing, and sintering of monodisperse  
288  $\text{TiO}_2$  powders, *Journal of the American Ceramic Society* 65 (12) (1982) C-199–C-201.  
289 doi:<https://doi.org/10.1111/j.1151-2916.1982.tb09948.x>.

- 290 [6] Y. Fu, Z. Jin, Z. Liu, W. Li, Preparation of ordered porous SnO<sub>2</sub> films by dip-drawing  
291 method with PS colloid crystal templates, *Journal of the European Ceramic Society*  
292 27 (5) (2007) 2223–2228. doi:<https://doi.org/10.1016/j.jeurceramsoc.2006.07.006>.
- 293 [7] E. S. A. Goerlitzer, R. N. Klupp Taylor, N. Vogel, Bioinspired photonic pig-  
294 ments from colloidal self-assembly, *Advanced Materials* 30 (28) (2018) 1706654.  
295 doi:<https://doi.org/10.1002/adma.201706654>.
- 296 [8] W. Gao, M. Rigout, H. Owens, Self-assembly of silica colloidal crystal thin  
297 films with tuneable structural colours over a wide visible spectrum, *Applied Sur-  
298 face Science* 380 (2016) 12–15, proceedings for International Conference on Sur-  
299 faces, Coatings and Nanostructured Materials (NANOSMAT-10, Manchester, UK).  
300 doi:<https://doi.org/10.1016/j.apsusc.2016.02.106>.
- 301 [9] A. K. Boehm, E. Ionescu, M. Koch, M. Gallei, Combining soft polysilazanes with melt-  
302 shear organization of core-shell particles: On the road to polymer-templated porous  
303 ceramics, *Molecules* 24 (19) (2019). doi:10.3390/molecules24193553.
- 304 [10] L. Gu, S. Xu, Z. Sun, J. Wang, Brownian dynamics simulation of the crystallization  
305 dynamics of charged colloidal particles, *J. Colloid Interf. Sci.* 350 (2) (2010) 409–416.  
306 doi:<https://doi.org/10.1016/j.jcis.2010.07.009>.
- 307 [11] M. Bini, G. Brancolini, V. Tozzini, Aggregation behavior of nanoparticles: re-  
308 visiting the phase diagram of colloids, *Front. Mol. Biosci.* 9 (2022) 986223.  
309 doi:[doi.org/10.3389/fmolb.2022.986223](https://doi.org/10.3389/fmolb.2022.986223).
- 310 [12] Y. Xia, B. Gates, Y. Yin, Y. Lu, Monodispersed colloidal spheres: Old  
311 materials with new applications, *Advanced Materials* 12 (10) (2000) 693–  
312 713. doi:[https://doi.org/10.1002/\(SICI\)1521-4095\(200005\)12:10<693::AID-  
313 ADMA693>3.0.CO;2-J](https://doi.org/10.1002/(SICI)1521-4095(200005)12:10<693::AID-ADMA693>3.0.CO;2-J).
- 314 [13] T. Hueckel, G. Hocky, J. Palacci, S. Sacanna, Ionic solids from common colloids, *Nature*  
315 580 (2020) 487–490. doi:[doi.org/10.1038/s41586-020-2205-0](https://doi.org/10.1038/s41586-020-2205-0).
- 316 [14] A. J. Kim, P. L. Biancaniello, J. C. Crocker, Engineering DNA-mediated colloidal crys-  
317 tallization, *Langmuir* 22 (5) (2006) 1991–2001. doi:10.1021/la0528955.

- 318 [15] D. Bochicchio, A. Videcoq, A. Studart, R. Ferrando, Compact and ordered colloidal  
319 clusters from assembly-disassembly cycles: a numerical study, *J. Colloid Interface Sci.*  
320 440 (2015) 198–203. doi:<https://doi.org/10.1016/j.jcis.2014.10.041>.
- 321 [16] T. Liu, B. VanSaders, S. C. Glotzer, M. J. Solomon, Effect of defective microstructure  
322 and film thickness on the reflective structural color of self-assembled colloidal crystals,  
323 *ACS Appl. Mater. Interfaces* 12 (2020) 9842–9850. doi:[doi.org/10.1021/acsami.9b22913](https://doi.org/10.1021/acsami.9b22913).
- 324 [17] F. Nakagawa, M. Saruyama, R. Takahata, R. Sato, K. Matsumoto, T. Teranishi,  
325 In situ control of crystallinity of 3D colloidal crystals by tuning the growth ki-  
326 netics of nanoparticle building blocks, *J. Am. Chem. Soc.* 13 (2022) 5871–5877.  
327 doi:<https://doi.org/10.1021/jacs.1c12456>.
- 328 [18] T. Liu, B. VanSaders, J. Keating, S. Glotzer, M. Solomon, Effect of particles of irreg-  
329 ular size on the microstructure and structural color of self-assembled colloidal crystals,  
330 *Langmuir* 37 (2021) 13300–13308. doi:<https://doi.org/10.1021/acs.langmuir.1c01898>.
- 331 [19] J. Lyklema, *Fundamentals of Interface and Colloid Science: Volume 1*, 1991.
- 332 [20] A. Tomilov, A. Videcoq, M. Cerbelaud, M. Piechowiak, T. Chartier, T. Ala-Nissila,  
333 D. Bochicchio, R. Ferrando, Aggregation in colloidal suspensions: evaluation of the role  
334 of hydrodynamic interactions by mean of numerical simulations, *J. Phys. Chem. B* (DOI:  
335 [10.1021/jp407247y](https://doi.org/10.1021/jp407247y)).
- 336 [21] L. Bergström, Hamaker constants for inorganic materials, *Adv. Colloid Interface Sci.* 70  
337 (1997) 125–169–A163. doi:[https://doi.org/10.1016/S0001-8686\(97\)00003-1](https://doi.org/10.1016/S0001-8686(97)00003-1).
- 338 [22] R. Hogg, T. Healy, D. Fuerstenau, Mutual coagulation of colloidal dispersions, *Trans.*  
339 *Faraday Soc.* 62 (1966) 1638–1651. doi:<https://doi.org/10.1039/TF9666201638>.
- 340 [23] C. T. Tran, B. Crespín, M. Cerbelaud, A. Videcoq, Brownian dynamics simulation on  
341 the gpu: Virtual colloidal suspensions, in: F. Jaillet, F. Zara, G. Zachmann (Eds.),  
342 *Workshop on Virtual Reality Interaction and Physical Simulation*, The Eurographics  
343 Association, 2015. doi:[10.2312/vriphys.20151332](https://doi.org/10.2312/vriphys.20151332).

344 [24] A.Stukowski, Visualization and analysis of atomistic simulation data with ovito -  
345 the open visualization tool, Modelling Simul. Mater. Sci. Eng. 18 (2010) 015012.  
346 doi:10.1088/0965-0393/18/1/015012.